

IMPROVED PERFORMANCE FOR AUTOMATIC BLOOD VESSELS DETECTION IN RETINAL IMAGES

¹Ram Kumar Choudhary, ²Vijay Kumar Sharma, ³Saroj Hiranwal

¹Student, ²Assistant Professor, ³Assistant Professor

¹Department of Computer Science and Engineering,

¹Rajasthan Institute of Engineering and Technology, Jaipur, India

Abstract: In this paper, the proposed approach employs a new methodology for segmenting the blood vessels from the retinal images more effectively. There is possibility for improvement in the process of detection blood vessels using segmentation techniques and then for validation classification methods can be implemented. The database of retinal images is taken from DRIVE and CHASE-DB1, these are available in open source for research. In this proposed work, segmentation of retinal images is compared with sobel and canny algorithms and further this is validated using parameters calculated from vesseness methods. The overall process is carried out in two stages. The first stag is to pre-processing of retinal images from database and to convert the color image into grey scale image and second stage will be for classification methods. From the experimental results, it has been observed that the proposed approach provides to decrease process time and increase accuracy in segmenting Retinal blood vessels.

Index Terms - Retina, Segmentation, DRIVE, CHASE-DB1, Canny operator, Sobel Operator.

I. INTRODUCTION

A new study shows that some morphological changes of retinal blood vessels in retinal images are symptoms of diseases such as diabetes, hypertension and cataracts. As a sign of various eye diseases, the length, width, diameter of blood vessels can be changed. For example, vessel interference that makes veins more, indicates abnormal contraction of retinal blood vessels, that the first stage of glaucoma or DR creates new blood vessels (small, thin, delicate and abnormal), and Often, permanent blood born of permanent blood can be harmful. Automated treatment extraction of retinal blood vessels is important for the diagnosis and treatment of various diseases like hypertension, obesity, cataract and diabetes mellitus. Diabetes Retinopathy a growing public health problem is the leading cause of blindness in the world. The correct address of the retinal blood vessel is important. In most of the retinal screening programs, blood vessels can be removed manually Figure 1 has captured a retinal image through eye-structure and a retinal imaging device. Many methods can be understood to split blood vessels [1].

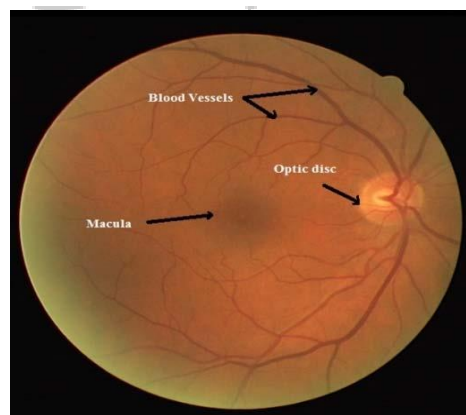
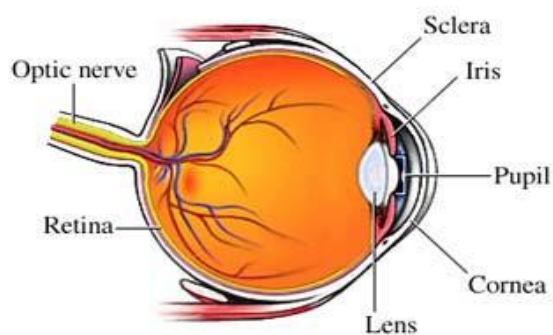


Fig. 1. (a) Anatomy of the eye (b) fundus image

As medical science in growing on engineering technology, this thesis proposes a technology to detect blood vessels in retinal images. To detect retinal blood vessels increases probability of finding many dieses in it.

Blood vessels can be detected by using image-processing techniques by reducing its process time and precision in results. Many techniques are introducing for detecting vessels from retinal, but there is scope of reducing time by means of implementing testing database by different process like Artificial Neural Network (ANN) etc.

The proposed work focus on detecting retinal vessels by using artificial neural network and compare it with previous works, for validation. This system gives more accurate and precious results on the parameter scaling of accuracy, precision etc.

II. PROPOSED TECHNIQUE AND METHODOLOGY

The flow of the image enhancement and feature extraction techniques are shown in Figure 2.

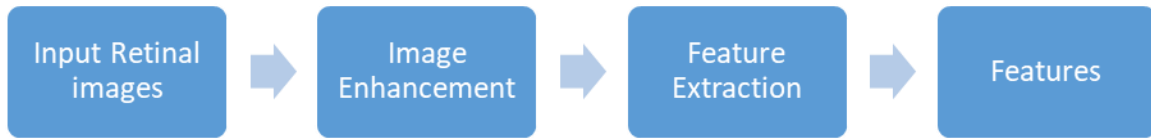


Fig.2. Flow of proposed methodology

The images are collected from image database available in open source and further analysis is carried out on these images. Finally, an optimal set of features are extracted from these images and used as input for the computational techniques. The input retinal images are discussed in this section and the image enhancement and the feature extraction techniques are analysed in next sections.

III. RETINAL IMAGE DATABASE

For analysis of retina images, the database is used from the open source. The open sources are DRIVE [30-32] and CHASE [33-35]. The number of images from these databases are 40 and 20 of 768x584 and 700x605 pixels respectively. Using Canon CR5 non-mydratric 3-CCD camera with a 45° field of view (FOV) for DRIVE dataset and Top Con TRV-50 camera with 35° FOV for CHASE image dataset. The format for images is JPEG and PPM.

DRIVE contains the test set contains colour fundus images, the FOV masks for the images, and two set of manually segmented monochrome ground truth images by two different specialists. The ground truth images of the first observer were used for measuring the performance of algorithms.

CHASE contains two sets of manually segmented monochrome ground truth images by two different specialists. The manually segmented images by the first human observer were used as the ground truth for evaluating the performance of the algorithms [34].

IV. FEATURE EXTRACTION

The textural features are another feature set used in this work. Since the abnormality was widely spread in the image, the textural orientation of each class is different, which aid in better classification accuracy. Six features based on first order histogram and seven features based on gray level co-occurrence matrix (GLCM) were used in this work.

The process used in pre-processing and vessel detection to achieve final results from various techniques used during these steps. This section of the thesis will explain the process steps of detecting vessels from retinal images of available image data sets. The whole process is divided into three steps as first is to input image from image datasets, second is its pre-processing using four steps in it and final step is to detect vessels from the image output from pre-processing steps. Next subsection is explanation of these in steps.

V. VESSELS DETECTION INPUT IN RGB IMAGE

The initial process of any program, which includes the input of colour (RGB) image to the system for analysis. Image from database of various sources will be taken as input to the process for further steps i.e. pre-processing.

Vessels Detection Stages

The stages for vessel Detection after pre-processing involves as follows:

- a) Vesselness Filter
- b) Enhancement Filter
- c) Adaptive Thresholding

The flow diagram for the image vessel detection technique is shown in Figure 3.

The detailed description of the individual stages is given below:

Stage 1. Vesselness Filter

The Frangi filter provides a measure of “Vesselness” (V) based on the eigenvalues of the Hessian matrix. Let λ_1 , λ_2 and λ_3 be the eigenvalues of the Hessian matrix sorted by increasing magnitude ($|\lambda_1|$, $|\lambda_2|$ and $|\lambda_3|$). For λ_2 or λ_3 greater than zero V is set to zero otherwise

$$V = \left(1 - e^{-\frac{R^2 a}{2a^2}}\right) e^{-\frac{R^2 a}{2a^2}} \left(1 - e^{-\frac{s^2}{2c^2}}\right) \quad (1)$$

Where

Ra is the ratio $|\lambda_2|/|\lambda_3|$,

Rb is the ratio of |I1| to the geometric mean of |I2| and |I3|,

S is the summation of |I1|, |I2| and |I3|, and

a, b, and c are normalizing constants taken to be 0.5, 0.5 and 0.5max(S) respectively.

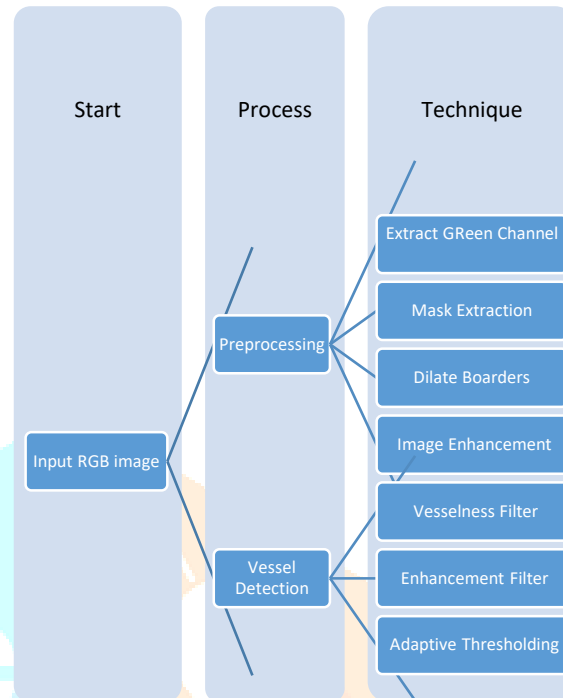


Fig.3. Process for blood vessel detection

Each patient provided informed consent. A single slab 3D TOF pulse sequence on a 1.5 T Sigma scanner was used for each acquisition. Images were acquired on a 512x192x64 grid and reconstructed on a 1024x768x128 grid. Magnetization transfer was used to suppress background signal.

The filter performance was analysed in terms of how well the vessel area were separated from the background. Separation was measured with the trapezoidal ROC curve (AUC). The mean and 10% confidence intervals (two tailed) for these curves were calculated by performing 2000 bootstraps. The ROC areas were calculated for the HessDiff filter, Frangi's filter and its three components, Ra, Rb, and S. A digital phantom was also used to test the relationship between the filters and the MIP algorithm [1, 7, 27]

Stage 2. Enhancement Filter

The improved Hessian multiscale enhancement filter, which combines the global grayscale information with the local geometric features. This improved filter can effectively reduce the number of the pseudo vessel structures and isolated noise points in the process of blood vessel enhancement. Therefore, the gray scale factor K added to Hessian multiscale filter is defined by:

$$K = \frac{1}{2} + \frac{1}{\pi} \arctan(\alpha X) \quad (2)$$

$$X = \frac{I(x,y) - Th}{\max(I(x,y))} \quad (3)$$

Where

$\alpha = 2$ is the smoothness factor of K.

Th = global adaptive threshold to determine whether I(x, y) is the vessel or not.

Stage 3. Adaptive Thresholding

Region based Thresholding is performed to convert the image to binary form. Too small a threshold value results in edge linking and a large threshold will result in edge segments. Hence, an optimum value of threshold is used which is 25% of the intensities contained in the image. To calculate the threshold value, the average of all the intensity values in an image is multiplied by 0.25. For example, an image with an average intensity value of 250 yields a threshold value of 63[10].

VI. IMPLEMENTATION OF PROPOSED TECHNIQUES

Output of Pre-Processing Stage

Input RGB Image and Green Channel Extraction

RGB image of retinal is taken from two sources as DRIVE and CHASE. The output images are shown in Figure 4. and Figure 5. shows the histogram of RGB image and gray scale green channel image obtained from green channel extraction stage.

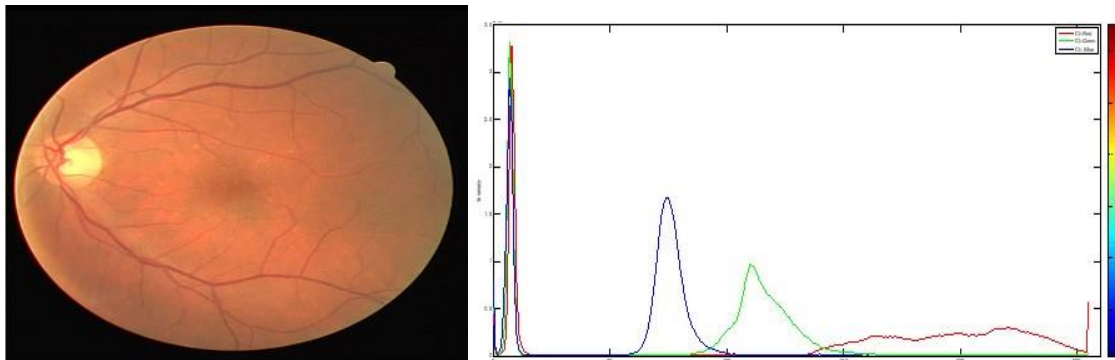


Fig. 4. RGB retinal image used for analysis & red, green and blue histogram of retinal image

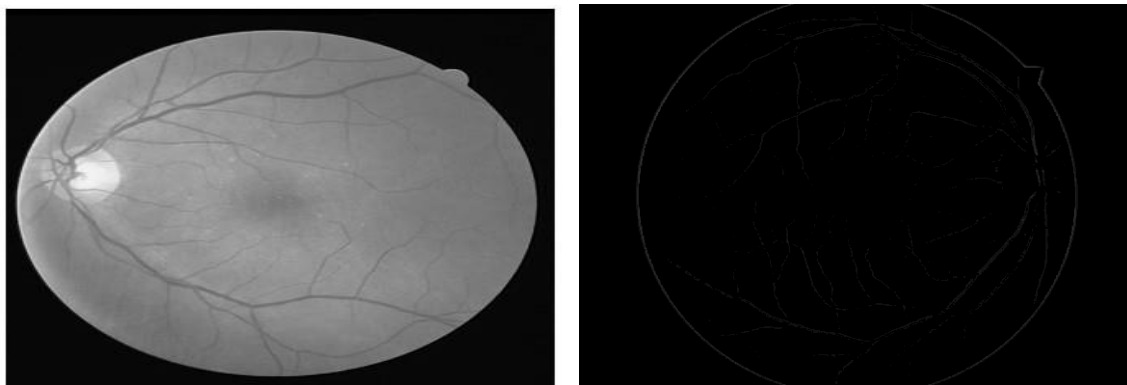


Fig.5. Gray scale green channel image & retinal image after mask extraction

Mask Extraction from Gray Scale Green Channel Image

As described in previous section masking of any retinal image is to separate image and background. The output obtained from this stage is shown in Figure 6.

Image Enhancement

Image enhancement and edge detection in pre-processing is done by using canny and sobel filters after mask extraction. Parameters are identified while edge detection for comparison are PR and Fmeasure.

Where; PR is Performance Ratio, Output image sets of DRIVE data and CHASE dataset is shown in Figure .6 respectively.

From CHASE database to output images and analysis are:

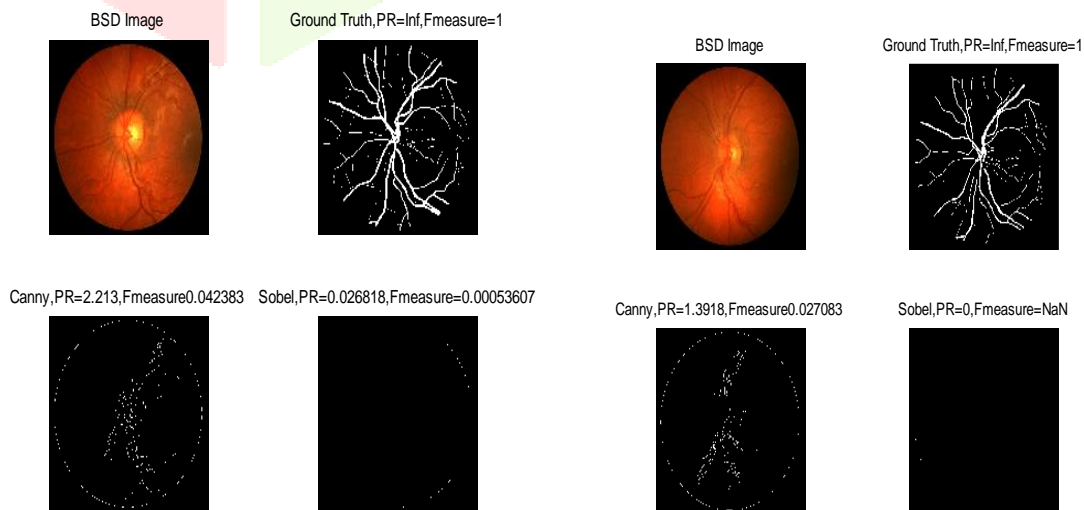


Fig.6. Output images from canny and sobel filters with comparison of pr and fmeasure of chase image database

$$\text{Sensitivity} = \frac{TP}{TP+FN} \quad (4)$$

$$\text{Specificity} = \frac{TN}{TN+FP} \quad (5)$$

$$\text{Accuracy} = \frac{TP+TN+FP+FN}{TP+TN+FP+FN} \quad (6)$$

$$\text{Precision} = \frac{TP}{TP+FP} \quad (7)$$

Where

Se= Sensitivity

Sp=Specificity

Ppv=Precision

Acc= Accuracy

Equation 4 to 7 represents the calculation for parameters used for analysis of results and to train system in classification, in these equations TP is true positive, TN is true negative, FN is false negative and FP is false positive. True Positive (TP) represents the output of system that shows that output is identified as infected and the manual segmented image or the input is also infected. That is mean that it's true that the image having positive results. Similarly, TN, FP and FN shows the results of classification and these values used to measure the sensitivity of work and how much accurate the results are being identified.

Table: 1. CHASE data analysis for 28 images

Image	Acc-Canny	Se-Canny	Sp-Canny	Acc-Sobel	Se-Sobel	Sp-Sobel
1	0.9221	0.0356	0.9886	0.93	0.000044853	0.9998
2	0.924	0.0246	0.9873	0.9342	0.000031717	0.9999
3	0.9173	0.0105	0.9918	0.923	0.000727640	0.9988
4	0.9287	0.0254	0.9899	0.9363	0.000049328	0.9996
5	0.912	0.024	0.9904	0.9183	0.000269850	0.9994
6	0.9323	0.0103	0.9927	0.9378	0.000016951	0.9992
7	0.9145	0.0163	0.9906	0.9218	0.000080118	0.9998
8	0.9322	0.0045	0.9944	0.9361	0.000000000	0.9988
9	0.9183	0.0046	0.996	0.92	0.000970800	0.9982
10	0.9336	0.0077	0.9929	0.9383	0.000052020	0.9983
11	0.912	0.0217	0.9847	0.9244	0.000000000	0.9999
12	0.9297	0.0323	0.9865	0.9405	0.000000000	1
13	0.9164	0.0163	0.993	0.9204	0.000811520	0.9986
14	0.9255	0.0103	0.9922	0.9306	0.000000000	0.9983
15	0.9139	0.0189	0.9886	0.923	0.000000000	1
16	0.929	0.0387	0.9822	0.9437	0.000000000	1
17	0.9178	0.0029	0.9965	0.9193	0.001200000	0.9983
18	0.9351	8.85E-04	0.9961	0.9372	0.000000000	0.9983
19	0.9053	0.0258	0.9872	0.9136		0.9986
20	0.9203	0.0349	0.9852	0.9316	0.000000000	0.9999
21	0.9209	0.0067	0.9958	0.9225	0.001300000	0.998
22	0.9352	0.008	0.9941	0.9385	0.000000000	0.9981
23	0.9227	0.002	0.9972	0.9243	0.000585220	0.9991
24	0.9255	0.0186	0.9909	0.9312	0.000031014	0.9984
25	0.9148	0.0222	0.9902	0.9217	0.000147260	0.9996
26	0.9182	0.0229	0.987	0.9286	0.000000000	1

27	0.9201	0.0048	0.9955	0.9221	0.001100000	0.998
28	0.918	0.0117	0.9911	0.9252	0.000000000	0.9999
Average	0.9219786	0.01653876	0.99102143	0.9283643	0.000264939	0.9991

Table 1 shows that the output reading of proposed work while working on CHASE database. Total 20 images are taken out of 40 for analysis of parameters discussed in previous section. Two segmentation methods are compared as Canny and Sobel and results are measured in its accuracy, sensitivity and specificity. Average accuracy of canny 0.92 or 92% where sober gives 0.93 or 93% accuracy. Similarly, Sensitivity is 0.165 and 0.00026 respectively and specificity comes with 0.991 and 0.999 for Canny and Sobel.

From DRIVE database to output images and analysis are shown in Fig.7:

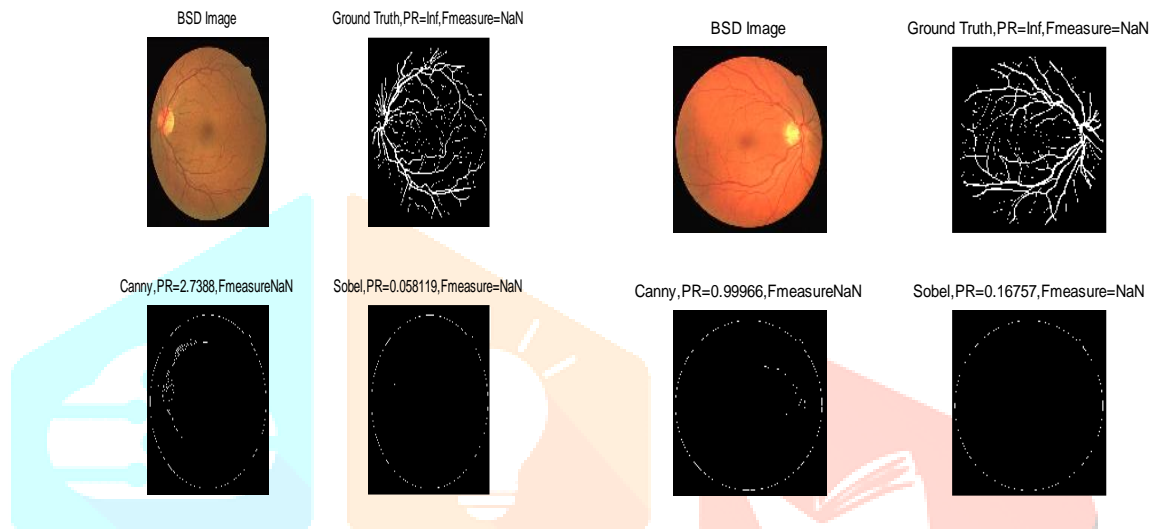


Fig.7. Output images from canny and sobel filters with comparison of pr and fmeasure of drive image database

VII. OUTPUT OF VESSEL DETECTION AND PARAMETER CALCULATION STAGE

The output parameters obtained for validation of results from retinal image datasets are shown in the performance result tables in this section.

Table: 2. DRIVE data analysis for 20 images

Image	Acc-Canny	Sp-Canny	Acc-Sobel	Sp-Sobel
1	0.9034	0.9034	0.9061	0.9061
2	0.8916	0.8916	0.8931	0.8931
3	0.8944	0.8944	0.8958	0.8958
4	0.9017	0.9017	0.9038	0.9038
5	0.8995	0.8995	0.9019	0.9019
6	0.8969	0.8969	0.8982	0.8982
7	0.9016	0.9016	0.9045	0.9045
8	0.9074	0.9074	0.9095	0.9095
9	0.9132	0.9132	0.9144	0.9144
10	0.9096	0.9096	0.9132	0.9132
11	0.9041	0.9041	0.9061	0.9061
12	0.9073	0.9073	0.9091	0.9091
13	0.8964	0.8964	0.8978	0.8978

14	0.9129	0.9129	0.9146	0.9146
15	0.915	0.915	0.926	0.926
16	0.9035	0.9035	0.9052	0.9052
17	0.9095	0.9095	0.911	0.911
18	0.9133	0.9133	0.9161	0.9161
19	0.9106	0.9106	0.9127	0.9127
20	0.9195	0.9195	0.9218	0.9218
Average	0.90557	0.90557	0.908045	0.908045

Table 2 shows that the output reading of proposed work while working on DRIVE database. Total 20 images are taken out of 40 for analysis of parameters. Two segmentation methods are compared as Canny and Sobel and results are measured in its accuracy, sensitivity and specificity. Average accuracy of Canny 0.90557 where Sobel gives 0.90804 accuracy. Similarly, Specificity comes with 0.90557 and 0.90804 for Canny and Sobel.

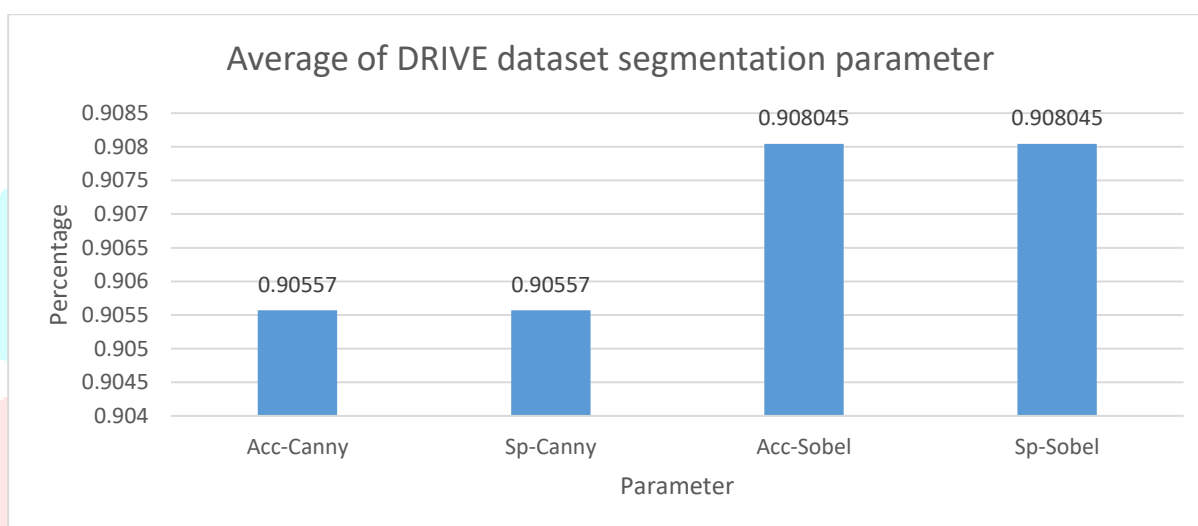


Fig. 8. Graphical representation of parameter of DRIVE database

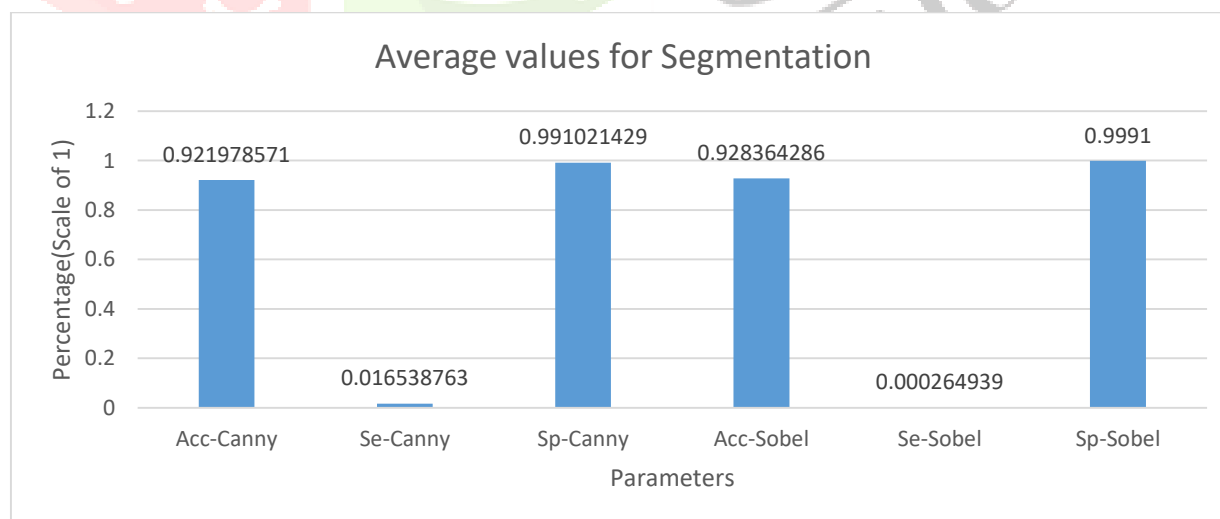


Fig. 9. Graphical representation of parameter of CHASE-DB database

For training the neural network, image 40 from the training set of DRIVE images was used. Whereas for the CHASE database, image 20 was used. The original authors' implementation of the algorithm used one input, three hidden layers each with 15 nodes and one output layer for both databases. In this thesis, one input, one hidden layer and one output layer were used. A neural

network using the authors' original configuration was also implemented, but the results were found to be poorer than with the new configuration. New configurations were chosen for both databases with the varying number of nodes in the hidden layer. For the DRIVE images, training is done with 20 nodes in a hidden layer, while for the CHASE images, training was done with 15 nodes. The training took around 25 minutes while simulation or testing required only 5 seconds to execute. For the DRIVE database, smaller amounts of nodes (e.g., 10 and 15) gave poorer classification accuracies and sensitivities than 20 nodes, which gave optimal performance results. Similarly, for CHASE images, hidden layer with 10 and 20 nodes were tested but the optimal results were obtained using 15 nodes in hidden layer.

The performance results shown in Tables 1 and 2 were obtained by applying the same threshold value Th for all the images in the same database (for DRIVE, 0.53 and for CHASE, 0.43 were used). These threshold values are different than the values used by the original author, which were 0.63 and 0.91 for DRIVE and CHASE images, respectively. When comparing with the original author's results, the implemented algorithm gives nearly same accuracy, specificity and negative predictive value (Table 3). The sensitivity and positive predictive value are smaller than original author's result. The implemented algorithm has slightly lower capability to detect thin vessels, which might be the reason for obtaining smaller values for Se and Ppv . The use of only one hidden layer rather than three layers in the neural network might explain the results obtained.

Table: 3. Comparison of performance results with original author

Image DATABASE	Method	Se	Sp	Acc
DRIVE	Soares et al. (2006) [5].	0.7332	0.9782	0.9466
	Xu et al. [6]	0.7406	0.9807	0.948
	Fraz et al. (2012) [11]	0.7406	0.9807	0.948
	Marin et al. (2011)	0.7067	0.9801	0.9452
	Mendonça et al. (2006) .	0.7344	0.9764	0.9463
	Martinez-Pérez et al. (2007)[10]	0.7246	0.9655	0.9344
	Lam et al. (2010) [9]	-	-	0.9472
	Azzopardi at al. [14] (2014)	0.7655	0.9704	0.9442
	Proposed method (For 40 Images)	0.7286	0.9857	0.948
CHASE_DB1	Method	Se	Sp	Acc
	Fraz et al. (2012) [11]	0.7224	0.9711	0.9469
	Azzopardi at al. [14] (2014)	0.7585	0.9587	0.9387
	Proposed method (For 20 Images)	0.753	0.996	0.9486

From Figures it is clearly see that. The proposed algorithm is compared with different retinal blood vessel segmentation algorithms. From the table, it can be observed that the segmentation accuracy of proposed methodology is greater when compared to the other existing methods for segmenting retinal blood vessels and it is also decrease the process time of computational images.

VIII. CONCLUSION

In this paper, it is carried out to detection of retinal blood vessels from retinal images taken from open source of DRIVE and CHASE_DB1. All work is classified into two segments as pre-processing and segmentation. we calculate the result on MAT lab image processing tool box by employing the three-method artificial neural network, canny and sobel from three different categories selected based on their better result which published in the literature. As the manual segmentation of blood vessels is so hard and time consuming. The main purpose algorithm is used to enhance the accuracy, sensitivity and specificity as compared to previous published performance result for blood vessels. It validates that the proposed algorithm works better than the work done in literature. These result shows that the use of engineering field in medical science will be play vital role in blood vessels detection in retinal images.

IX. REFERENCES

- [1] Elbalaoui, M. Fakir, K. Taifi and A. Merbouha, "Automatic Detection of Blood Vessel in Retinal Images," 2016 13th International Conference on Computer Graphics, Imaging and Visualization (CGiV), Beni Mellal, 2016, pp. 324-332.
- [2] Aarti and N. Gupta, "Performance evaluation of retinal vessel segmentation using a combination of filters," 2016 2nd International Conference on Next Generation Computing Technologies (NGCT), Dehradun, 2016, pp. 725-730.
- [3] Al-Rawi, Mohammed, Munib Qutaishat, and Mohammed Arrar. "An improved matched filter for blood vessel detection of digital retinal images." *Computers in Biology and Medicine* 37.2 (2007): 262-267.
- [4] Azzopardi, George, et al. "Trainable COSFIRE filters for vessel delineation with application to retinal images." *Medical image analysis* 19.1 (2015): 46-57.
- [5] K. Firdausy and K. Widhia Oktoeberza, "Segmentation of optic disc using dispersive phase stretch transform," 2016 6th International Annual Engineering Seminar (InAES), Yogyakarta, 2016, pp. 154-158.
- [6] Frangi, Alejandro F., et al. "Multiscale vessel enhancement filtering." *International Conference on Medical Image Computing and Computer-Assisted Intervention*. Springer Berlin Heidelberg, 1998.
- [7] M. M. Fraz et al., "An Ensemble Classification-Based Approach Applied to Retinal Blood Vessel Segmentation," in *IEEE Transactions on Biomedical Engineering*, vol. 59, no. 9, pp. 2538-2548, Sept. 2012.
- [8] M. Frucci, D. Riccio, G. S. d. Baja and L. Serino, "Effective Retinal Blood Vessel Detection Using Only Directional Information," 2015 11th International Conference on Signal-Image Technology & Internet-Based Systems (SITIS), Bangkok, 2015, pp. 583-590.
- [9] H. Gongt, Y. Li, G. Liu, W. Wu and G. Chen, "A level set method for retina image vessel segmentation based on the local cluster value via bias correction," 2015 8th International Congress on Image and Signal Processing (CISP), Shenyang, 2015, pp. 413-417.
- [10] Hoover, A. D., Valentina Kouznetsova, and Michael Goldbaum. "Locating blood vessels in retinal images by piecewise threshold probing of a matched filter response." *IEEE Transactions on Medical Imaging* 19.3 (2000): 203-210.
- [11] M. A. Hussain, A. Bhuiyan and K. Ramamohanarao, "Disc segmentation and BMO-MRW measurement from SD-OCT image using graph search and tracing of three bench mark reference layers of retina," 2015 IEEE International Conference on Image Processing (ICIP), Quebec City, QC, 2015, pp. 4087-4091.
- [12] J. Justin, R. Vanithamani and R. R. Christina, "Comparative study of retinal vessel segmentation methods," 2015 IEEE International Conference on Computational Intelligence and Computing Research (ICCIC), Madurai, 2015, pp. 1-3.
- [13] S. P. K. Karri, N. Garai, D. Nawn, S. Ghosh, D. Chakraborty and J. Chatterjee, "Retinal layer delineation through learning of tissue photon interaction in optical coherence tomography," 2016 IEEE Students' Technology Symposium (TechSym), Kharagpur, 2016, pp. 46-51.
- [14] B. S. Y. Lam, Y. Gao and A. W. C. Liew, "General Retinal Vessel Segmentation Using Regularization-Based Multiconcavity Modeling," in *IEEE Transactions on Medical Imaging*, vol. 29, no. 7, pp. 1369-1381, July 2010.
- [15] D. Marin, A. Aquino, M. E. Gegundez-Arias and J. M. Bravo, "A New Supervised Method for Blood Vessel Segmentation in Retinal Images by Using Gray-Level and Moment Invariants-Based Features," in *IEEE Transactions on Medical Imaging*, vol. 30, no. 1, pp. 146-158, Jan. 2011.
- [16] Martinez-Perez, M. Elena, et al. "Segmentation of blood vessels from red-free and fluorescein retinal images." *Medical image analysis* 11.1 (2007): 47-61.
- [17] Mendonca, Ana Maria, and Aurelio Campilho. "Segmentation of retinal blood vessels by combining the detection of centerlines and morphological reconstruction." *IEEE transactions on medical imaging* 25.9 (2006): 1200-1213.
- [18] S. Morales, K. Engan, V. Naranjo and A. Colomer, "Retinal Disease Screening Through Local Binary Patterns," in *IEEE Journal of Biomedical and Health Informatics*, vol. 21, no. 1, pp. 184-192, Jan. 2017.
- [19] F. Nabi, H. Yousefi and H. Soltanian-Zadeh, "Segmentation of major temporal arcade in angiography images of retina using generalized hough transform and graph analysis," 2015 22nd Iranian Conference on Biomedical Engineering (ICBME), Tehran, 2015, pp. 287-292.
- [20] S. Naz, A. Ahmed, M. U. Akram and S. A. Khan, "Automated segmentation of RPE layer for the detection of age macular degeneration using OCT images," 2016 Sixth International Conference on Image Processing Theory, Tools and Applications (IPTA), Oulu, 2016, pp. 1-4.
- [21] J. Novosel, S. Yzer, K. A. Vermeer and L. J. van Vliet, "Segmentation of Locally Varying Numbers of Outer Retinal Layers by a Model Selection Approach," in *IEEE Transactions on Medical Imaging*, vol. 36, no. 6, pp. 1306-1315, June 2017.
- [22] Owen, Christopher G., et al. "Measuring retinal vessel tortuosity in 10-year-old children: validation of the Computer-Assisted Image Analysis of the Retina (CAIAR) program." *Investigative ophthalmology & visual science* 50.5 (2009): 2004-2010.
- [23] Rangayyan, Rangaraj M., et al. "Detection of blood vessels in the retina with multiscale Gabor filters." *Journal of Electronic Imaging* 17.2 (2008): 023018-023018.
- [24] A. Razban, K. Mahjoory and M. Nooshyar, "Segmentation of retinal blood vessels by means of 2D Gabor wavelet and fuzzy mathematical morphology," 2016 2nd International Conference of Signal Processing and Intelligent Systems (ICSPIS), Tehran, 2016, pp. 1-5.
- [25] A. Sharma and S. Rani, "An automatic segmentation & detection of blood vessels and optic disc in retinal images," 2016 International Conference on Communication and Signal Processing (ICCSP), Melmaruvathur, 2016, pp. 1674-1678.

- [26] J. V. B. Soares, J. J. G. Leandro, R. M. Cesar, H. F. Jelinek and M. J. Cree, "Retinal vessel segmentation using the 2-D Gabor wavelet and supervised classification," in IEEE Transactions on Medical Imaging, vol. 25, no. 9, pp. 1214-1222, Sept. 2006.
- [27] Staal, Joes, et al. "Ridge-based vessel segmentation in color images of the retina." IEEE transactions on medical imaging 23.4 (2004): 501-509.
- [28] A. Stankiewicz, T. Marciniak, A. Dąbrowski, M. Stopa, E. Marciniak and A. Michalski, "Matching 3D OCT retina images into super-resolution dataset," 2016 Signal Processing: Algorithms, Architectures, Arrangements, and Applications (SPA), Poznan, 2016, pp. 130-137.
- [29] Z. Waheed, A. Waheed and M. U. Akram, "A robust non-vascular retina recognition system using structural features of retinal image," 2016 13th International Bhurban Conference on Applied Sciences and Technology (IBCAST), Islamabad, 2016, pp. 101-105.
- [30] J.J. Staal, M.D. Abramoff, M. Niemeijer, M.A. Viergeever, B. van Ginneken, "Ridge based vessel segmentation in color images of the retina", IEEE Transactions on Medical Imaging, 2004, vol. 23, pp. 501-509.
- [31] M. Niemeijer, J.J. Staal, B. van Ginneken, M. Loog, M.D. Abramoff, "Comparative study of retinal vessel segmentation methods on a new publicly available database", in: SPIE Medical Imaging, Editor(s): J. Michael Fitzpatrick, M. Sonka, SPIE, 2004, vol. 5370, pp. 648-656.
- [32] Budai, Attila; Bock, Rüdiger; Maier, Andreas; Hornegger, Joachim; Michelson, Georg. Robust Vessel Segmentation in Fundus Images. International Journal of Biomedical Imaging, vol. 2013, 2013
- [33] Attila Budai, Joachim Hornegger, Georg Michelson: Multiscale Approach for Blood Vessel Segmentation on Retinal Fundus Images. In Invest Ophthalmol Vis Sci 2009;50: E-Abstract 325, 2009.
- [34] Jan Odstrcilik, Jiri Jan, Radim Kolar, and Jiri Gazarek. Improvement of vessel segmentation by matched filtering in colour retinal images. In IFMBE Proceedings of World Congress on Medical Physics and Biomedical Engineering, pages 327 - 330, 2009.
- [35] Jan Odstrcilik, Radim Kolar, Attila Budai, Joachim Hornegger, Jiri Jan, Jiri Gazarek, Tomas Kubena, Pavel Cernosek, Ondrej Svoboda, Elli Angelopoulou, „Retinal vessel segmentation by improved matched filtering: evaluation on a new high-resolution fundus image database,“ IET Image Processing, Volume 7, Issue 4, June 2013, pp.373-383.

